100 days of ELF/VLF generation via HF heating with HAARP

M. B. Cohen[1] and M. Gołkowski[2]

Received 20 June 2013; revised 6 August 2013; accepted 10 September 2013.

[1] Extremely low frequency/very low frequency (ELF/VLF) radio waves are difficult to generate with conventional antennas. Ionospheric high frequency (HF) heating facilities generate ELF/VLF waves via modulated heating of the lower ionosphere. HF heating of the ionosphere changes the lower ionospheric conductivity, which in the presence of natural currents such as the auroral electrojet creates an antenna in the sky when heating is modulated at ELF/VLF frequencies. We present a summary of nearly 100 days of ELF/VLF wave generation experiments at the 3.6 MW High Frequency Active Auroral Research Program (HAARP) facility near Gakona, Alaska, at a variety of ELF/VLF frequencies, seasons, and times of day. We present comprehensive statistics of generated ELF/VLF magnetic fields observed at a nearby site, in the 500–3500 Hz band. Transmissions with a specific HF beam configuration (3.25 MHz, vertical beam, amplitude modulation) are isolated so the data comparison is self-consistent, across nearly 5 million individual measurements of either a tone or a piece of a frequency-time ramp. There is a minimum in the average generation close to local midnight. It is found that generation during local nighttime is on average weaker but more highly variable, with a small number of very strong generation periods. Signal amplitudes from day to day may vary by as much as 20–30 dB. Generation strengthens by ∼5 dB during the first ∼30 min of transmission, which may be a signature of slow electron density changes from sustained HF heating. Theoretical calculations are made to relate the amplitude observed to the power injected into the waveguide and reaching 250 km. The median power generated by HAARP and injected into the waveguide is ∼0.05–0.1 W in this baseline configuration (vertical beam, 3.25 MHz, amplitude modulation) but may have generated hundreds of watts for brief durations. Several efficiency improvements have improved the ELF/VLF wave generation efficiency further.

Citation: Cohen, M. B. and M. Gołkowski (2013), 100 days of ELF/VLF generation via HF heating with HAARP, *J. Geophys. Res. Space Physics*, *118*, doi:10.1002/jgra.50558.

1. Introduction

[2] Extremely low frequency (ELF, 0.3–3 kHz) and very low frequency (VLF, 3–30 kHz) radio waves are difficult to generate with conventional antennas. Because the free space wavelengths (10–1000 km) are so much longer than a practically realizable vertical monopole antenna, the radiation efficiency is exceedingly small. As described by *Watt* [1967], reasonable radiation can only be achieved via impedance-matched loading at the feed point, to cancel out the reactance of the antenna. But this only works in a narrow frequency band, which limits these transmitters to bandwidths of a few hundred hertz, at most. On the other hand, a long horizontal antenna above the surface is limited by the image current below the conducting ground, which severely curtails the efficiency.

[3] Nonetheless, ELF/VLF waves are useful for long distance and sub-sea surface communications, geophysical prospecting, and geophysical experiments via controlled radio wave production. At these frequencies, the lower ionosphere (60–90 km) acts as an excellent reflector, guiding energy to global distances with small attenuation rates. Some VLF energy does escape the ionosphere, however [*Cohen and Inan*, 2012; *Cohen et al.*, 2012b]. ELF/VLF waves also penetrate into conducting seawater and ground via the skin effect. ELF/VLF waves from lightning entering the magnetosphere are known to impact radiation-belt electrons [*Bortnik et al.*, 2006; *Peter and Inan*, 2007; *Cotts et al.*, 2011], which can be studied via controlled generation, as with the Siple Station experiment [*Helliwell and Katsufrakis*, 1974]. Waves from powerful VLF transmitters are known to generate ionospheric heating [*Inan*, 1990; *Graf et al.*, 2011]. See *Barr et al.* [2000] for a review of some of these topics.

[1]School of Electrical and Computer Engineering, Georgia Institute of Technology, Atlanta, Georgia, USA.
[2]Department of Electrical Engineering, University of Colorado Denver, Denver, Colorado, USA.

Corresponding author: M. B. Cohen, School of Electrical and Computer Engineering, Georgia Institute of Technology, 777 Atlanta Drive NW, Atlanta, GA 30332, USA. (morris.cohen@ece.gatech.edu)

2169-9380/13/10.1002/jgra.50558

[4] Powerful high frequency (HF, 3–30 kHz) heating facilities have, since the first observations by *Getmantsev et al.* [1974], provided a unique way to generate ELF/VLF waves, using the ionosphere to nonlinearly convert HF power to ELF/VLF power. A phased array of HF antennas on the ground form a focused beam of HF radio waves which heat the ionospheric plasma in the *D*-region and alter the plasma conductivity. The HF heating can be modulated at an ELF/VLF rate, so that the conductivity rises and falls accordingly. In the presence of natural ionospheric currents such as the auroral electrojet, this is effectively like modulating the value of a resistor with a steady voltage across it, creating an antenna in the sky. A number of facilities have engaged in this research, an early prominent example being the European Incoherent Scatter facility in Tromso, Norway, with a long series of studies in the 1980s and 1990s [*Stubbe et al.*, 1981; *Barr and Stubbe*, 1984; *Rietveld et al.*, 1984; *Barr et al.*, 1985a; *Rietveld et al.*, 1987; *Barr et al.*, 1987; *Barr and Stubbe*, 1991, 1997; *Barr*, 1998]. Modulated HF heating also produces radiation in the Schumann resonance range [*McCarrick et al.*, 1990].

[5] The High Frequency Active Auroral Research Program (HAARP), located near Gakona, Alaska, was constructed in 1999 and reached its final operating stage in 2007. It consists of 180 crossed 10 kW elements, radiating a total of 3.6 MW, with effective radiating power between 300 MW and 3 GW and between 2.75 and 10 MHz. It is the most powerful HF heating facility that has been constructed. A number of breakthroughs in ELF/VLF generation have taken place since it was completed in February 2007. Generated ELF/VLF signals detected at ∼700 km distance were found to be useful as a diagnostic of the auroral electrojet direction [*Cohen et al.*, 2008a], with signals detected surprisingly strongly as far as 4400 km distance [*Cohen et al.*, 2010c] following a weaker detection at that distance prior to the final power upgrade [*Moore et al.*, 2007]. HAARP ELF/VLF signals were observed to be injected into space [*Piddyachiy et al.*, 2008] and detected at the geomagnetic conjugate region [*Gołkowski et al.*, 2008], as well as a second echo near HAARP [*Gołkowski et al.*, 2009], with the received signals useful as a magnetospheric probing source [*Gołkowski et al.*, 2010]. Using the rapid steering ability of HAARP to modulate the beam spatially, instead of pointing the beam vertically and modulating in time, generated 7–11 dB higher amplitudes and gave directional abilities [*Cohen et al.*, 2008b, 2010b, 2010a, 2011]. The connection between HAARP ELF/VLF amplitudes and natural conditions was investigated [*Jin et al.*, 2011], as were the properties of the communications channel [*Jin et al.*, 2013]. The HF beam can also be divided into two, and the so-called dual-beam modulated heating is being used for characterizing the *D*-region of the ionosphere [*Moore and Agrawal*, 2011; *Agrawal and Moore*, 2012; *Gołkowski et al.*, 2013]. The importance of HF frequency and beam shape was investigated [*Cohen et al.*, 2012a], as well as the effect of modulation waveform [*Jin et al.*, 2012]. A novel analysis technique, which provides time of arrival information from a transmitted ELF/VLF frequency-time ramp enables location of the height of the generating region [*Fujimaru and Moore*, 2011; *Moore et al.*, 2012]. A pulsed heating and modulation technique in combination with direct HF observations allows characterization of the *D*-region absorption [*Langston and Moore*, 2013].

[6] The aforementioned papers yielded many exciting results but largely conducted individual experiments, presenting the results of some limited hours of targeted efforts. In this paper, we construct and analyze a large catalog of the received amplitudes from ELF/VLF generation at a nearby site.

2. Description of Data

[7] ELF/VLF data are taken with the Atmospheric Weather Electromagnetic System for Observation Modeling and Education (AWESOME) receiver, described by *Cohen et al.* [2010c]. The receiver consists of two crossed air-core magnetic loop antennas measuring the two horizontal components of the magnetic field, sensitive to signals in the fT range, across a frequency band between 300 Hz and 47 kHz. The data are sampled at 100 kHz, at 16 bits, with 100 ns absolute time accuracy thanks to GPS synchronization. Data are saved continuously during HAARP campaigns at a number of receivers across Alaska and elsewhere, but we focus here on recordings made at Chistochina (located at 62.613°N, 144.624°W), a receiver placed ∼37 km from the HAARP HF array (located at 62.39°N, 145.15°W). Due to the site's proximity to HAARP, ELF/VLF signals were clearly observed for nearly all transmissions. When integrating for a second in the few kilohertz range, the detection noise floor at Chistochina is no higher than –60 dB-pT, which is below even the weakest generated HAARP signals.

[8] HAARP was especially active for ELF/VLF wave generation experiments between February 2007 and August 2008, immediately following completion of construction, though ELF/VLF experiments continue to the present day. During that initial 19 month period, there were more than 100 days on which HAARP was used for ELF/VLF wave generation. Most days included 5–12 h of continuous transmissions.

[9] HAARP is in general capable of modulating the HF carrier with an arbitrary ELF/VLF frequency-time signature, including constant frequency tones, frequency sweeping ramps, or chirps. The experiments during this period were largely focused on injecting ELF/VLF waves into space, known as one-hops (if received at the conjugate region) or two-hops (if reflected and received back near HAARP). The purpose was to trigger nonlinear wave growth and emissions, as first observed by *Inan et al.* [2004]. However, injection into space and reception of a magnetospheric component only occurred on ∼10% of days, being limited by magnetosphere and plasmasphere conditions [*Gołkowski et al.*, 2011], and typically lasted ∼30 min when it did occur. As such, for the bulk of the experimental time, HAARP operated in a diagnostic mode, which included a variety of types of signals. It was not known what type of frequency-time signal would generate two-hops, so the idea was to transmit a variety of frequencies and formats and shift to one of a few special formats when two-hops were observed in real time. For instance, the first one-hop detection made after the construction of HAARP resulted from a tilted sinusoidal frequency-time ramp known as a "snake ramp" [*Gołkowski et al.*, 2008].

[10] While ground observation of HAARP-induced magnetospheric emissions was relatively rare, generation of ELF/VLF waves in the Earth-ionosphere waveguide was

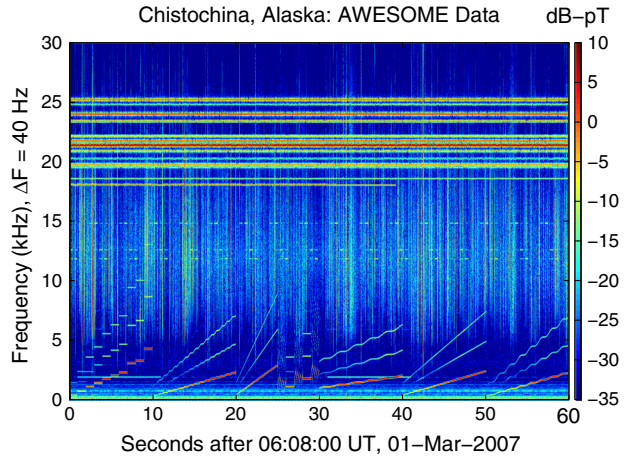

Figure 1. An example of HAARP ELF/VLF signals detected at Chistochina, AK, 37 km away. The magnetic field is binned into 25 ms segments ($\Delta f = 40$ Hz), and the spectrum of each bin is shown in the color scale. Vertical lines are impulsive (1 ms long) signals from global lightning. Horizontal lines between 19 and 26 kHz are VLF transmitters for naval communications. The pulses between 11 and 15 kHz are the Russian "Alpha" navigation system. The HAARP signals appear below 10 kHz and consist of tones, ramps, and chirps, at both a fundamental frequency, at harmonics from the nonlinear HF heating process.

always present, making these experiments a rich source of data for comprehensive statistical analysis. Figure 1 shows an example of HAARP-generated waves from a diagnostic format. This sequence, lasting 60 s, was cycled and included tones at many frequencies, ramps, and chirps, between 0.5 and 4 kHz. HAARP-generated signals typically include multiple harmonics, due to the fact that the HF heating process is highly nonlinear, but in this paper we focus only on the first harmonic. The HAARP-generated signals are seen in the context of the general ELF/VLF environment which includes lightning-generated radio atmospherics (vertical lines), Russian Alpha transmitting beacons (pulses between 11 and 14 kHz), and VLF Navy transmitters (horizontal lines between 18 and 27 kHz). In the background is a weaker 2 kHz signal from a now dismantled HF heating facility called high-power auroral simulation, which was located near Fairbanks, Alaska.

[11] Since transmission formats similar to that shown in Figure 1 were used for the bulk of the time during the 19 month experiments, there is sufficient consistency in the transmissions, for meaningful comparison across the entire data set. In order to compile statistics, we created an analysis tool that sequentially goes through the data and extracts the amplitudes of the generated signals as observed at Chistochina. For constant frequency tones, the signals are mixed down to baseband by multiplying with a complex exponential $e^{-j\omega t}$, where $\omega = 2\pi f$ is the frequency of the tone. The resulting signal, now shifted to baseband, is integrated over the full duration of the pulse, to maximize the SNR and interference rejection. The integral is computed in phasor form, on each of two channels, so the L2 norm of the two phasor amplitudes is taken as the total horizontal magnetic field. There is useful information in the phase of the phasor complex numbers, as well, but we do not consider that here. The L2 norm is independent of the polarization, so it is a better measure of the generated magnetic field energy than either the radial or the azimuthal component taken on their own. For other types of frequency-time signals, such as ramps and chirps, the same process is followed, except that ω is a function of time. The ramps are divided up into small pieces 0.1 s long, referred to here as a "ramp element," so that each ramp element includes a bandwidth of 10–100 Hz, depending on the sweep rate of the ramp. The chirps are excluded from the analyses, because their frequency changes too quickly.

[12] The resulting amplitudes are cataloged according to ELF frequency, date, and time. Most of the amplitudes correspond to when HAARP is transmitted in a specific mode, using an HF frequency of either 2.75 or 3.25 MHz, with amplitude modulation and a narrow focused beam. The remaining transmissions were part of various individual experiments that involved tilting the beam, steering or spinning the beam, dividing the beam into two, widening the beam, or operating at a higher HF frequency. These other experiments were all excluded from the catalog presented here, as the beam manipulation all impacts the generation amplitudes (see in particular *Cohen et al.* [2010b, 2012a]). The resulting catalog is self-consistent, containing only amplitudes of observations of HAARP-generated ELF/VLF waves from a single HF beam with conventional AM modulation. The remaining variations in signal amplitudes are due almost entirely to natural changes in the auroral electrojet and the ionosphere, both of which strongly impact generation of ELF/VLF waves with HF heating. In total, the catalog consists of 846 h of transmissions spread over 91 days, ∼712,000 tones (typically 1–3 s long), and ∼4.2 million ramp elements (each 0.1 s). The data set is thus sufficiently large and uniformly spread that selection bias is not a concern.

[13] Figure 2 shows the distribution of times of the day (30 min bins, as shown in the left panel) and ELF/VLF frequencies (250 Hz bins, as shown in the right panel) of the catalog. We show this distribution to demonstrate that experiments took place at all times of day and were not confined to just daytime or just nighttime. Hence, we have reliable diurnal generation statistics. In particular, the frequency range spanning 500–3500 Hz was transmitted reliably on nearly every single day, in large part because of frequency-time ramps covering that range, which were very common

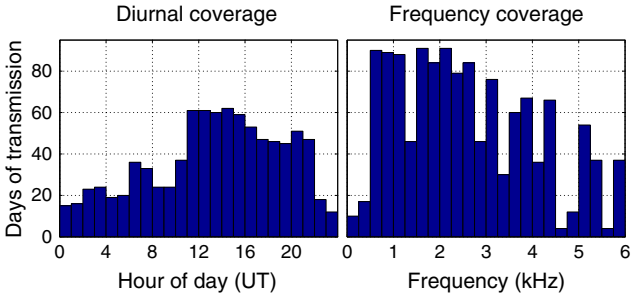

Figure 2. The (left) diurnal and (right) frequency coverages and the number of days within this data set in which HAARP is transmitted at that time or frequency.

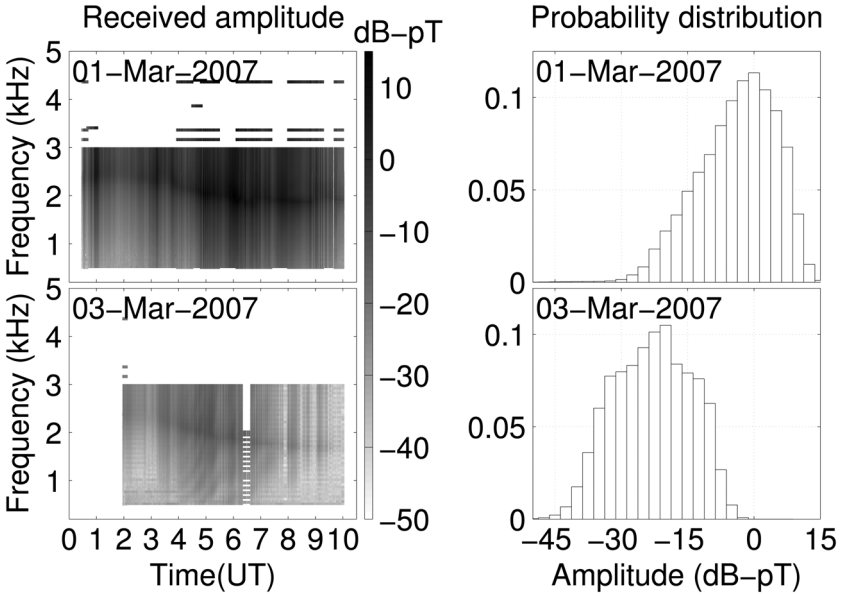

Figure 3. (left) Amplitude of every HAARP-generated tone and pulse during two selected days, (top) 1 March 2007 and (bottom) 3 March 2007, as a function of time and frequency. (right) The histogram of tone amplitudes for the same 2 days.

in the diagnostic formats. As such, the remainder of the statistical analysis in this paper focuses on this band of frequencies. All daytime and nighttime designations for the rest of this paper refer to the conditions at 75 km altitude above HAARP.

[14] The majority of campaign days included transmission for a ∼10 h period between ∼11 and ∼21 UT, which (close to the equinox) includes the period from the very early morning until early afternoon. During wintertime, this was roughly half nighttime, and during summertime, it was entirely daytime. However, a significant number of campaign days were also run between 23 and 9 UT.

3. Observations

[15] We first present an exploratory comparison of 2 days of observations before discussing comprehensive statistics of the entire data set. Figure 3 shows the amplitudes of HAARP signals on 1 March 2007 (top) and 3 March 2007 (bottom). Recordings on 1 March 2007 were made from 00:30 until 10:00 UT and between 02:00 and 10:00 UT on 3 March 2007. Although separated by just 2 days and transmissions were made during the same part of the day, the generation conditions were radically different. 1 March 2007 was one of the strongest days of transmission that has been observed since HAARP was completed, particularly close to 06:00 UT, for which the results were previously described by *Cohen et al.* [2008a] and for which signals were strongly observed at Midway Atoll, 4400 km away [*Cohen et al.*, 2010c]. On the other hand, 3 March 2007 saw some of the weakest generation conditions.

[16] The two left panels of Figure 3 show the amplitudes of all generated tones and ramps during the recordings for the 2 days. Each tone or ramp element is represented by a dot on the figure, with the amplitude indicated via the color. The transmitted formats on these 2 days included a large number of 500 Hz to 3.5 kHz ramps, at 500 Hz/s, so the frequency response of HAARP ELF/VLF generation is being sampled repeatedly over many hours. On both days, a peak in the frequency response can be seen, starting at ∼2.3 kHz and descending down to ∼1.9 kHz toward the end of the recording. These result from cavity resonance between the Earth and the ionosphere [*Stubbe et al.*, 1981; *Cohen et al.*, 2012a], which are particularly strong close to the transmitter and will be discussed more later. The resonance frequency drops as the Sun sets over the ionosphere which greatly decreases the ionization, leading to a rise in the ionospheric reflection height and absorption altitude range.

[17] The right panels of Figure 3 show the distribution of ELF/VLF amplitudes on these 2 days. On 1 March 2007, most of the transmissions were received between –15 and 10 dB-pT. On 3 March 2007, the range of amplitudes spans –40 through –10 dB-pT. These 2 days demonstrate a difference in generation conditions of ∼30 dB, likely due to either a weaker auroral electrojet on 3 March 2007 or an ionospheric profile less favorable for generation. *Rietveld et al.* [1987] and *Jin et al.* [2011] observe and model the connection between generated amplitudes and geophysical conditions, so we do not elaborate further here. All amplitudes presented here are uncorrected for any geophysical measurement, so the natural variation in signal strength is largely due to the natural variation in the generation conditions.

[18] The left panel of Figure 4 shows the histogram of all tones and ramp elements received, over the entire 19 month period, in logarithmic values. The tones are shown in blue and the ramp elements in red. The median signal strength for tones is –12.9 dB-pT and for the ramp elements is –11.8 dB-pT. The standard deviation of the logarithmic amplitude values is 12.9 dB-pT for the tones and 9.8 dB-pT for the ramp elements. The strongest tone in this catalog was just over 24 dB-pT (11.8 pT) and was transmitted for

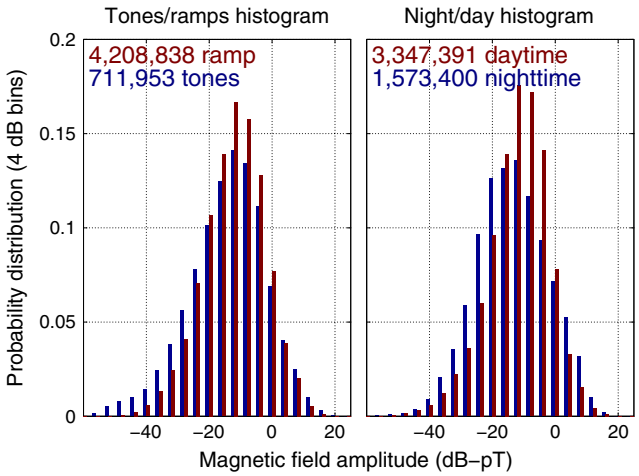

Figure 4. (left) The distribution of all amplitudes of tones (blue) and ramp elements (red) received at Chistochina over the 19 month period, between 0.5 and 3 kHz, a total number of ∼712,000 tones and 3,600,000 ramp elements. (right) Distribution of night (blue) and day (red) amplitudes, a total number of ∼3,350,000 nighttime and ∼1,157,000 daytime.

2.75 s on 12 March 2008, at 07:23:59:11 UT, at a frequency of 1875 Hz. The signals during the few minutes around this tone were so strong that harmonics could be seen as high as 50 kHz. At the same time, a receiver in Juneau, 700 km distance, picked up the sixth and seventh harmonics quite clearly and detected the fundamental with an amplitude of –16 dB-pT. This is ∼15 dB higher than the strong signals that were detected on 1 March 2007, reported by *Cohen et al.* [2008a, 2010c] and shown in Figure 3. We elaborate on the power levels associated with these emissions later.

[19] The distribution of the tones and ramp elements is not precisely the same but is quite similar. Overall, the ramp elements have a slightly higher median value. Since the ramp elements have a shorter duration, there is a slightly higher detection noise floor, so there are fewer weak ramp elements compared to tones. In addition, the tones do not evenly sample the frequency range, since they are chosen at discrete values, whereas each ramp covers an entire frequency band. Since there is a strong frequency dependence of ELF/VLF generation with HF heating, there may be some selection bias from the distribution of tone frequencies. However, we also cannot rule out the possibility that ramps are slightly more efficient than tones for ELF/VLF wave generation, due to the fact that the frequency is constantly changing. Consideration of this possibility is outside the scope of this paper. Since there are about 6 times more ramp elements than tones, the subsequent measurements are largely driven by the ramps, but none of the remaining results presented herein are significantly different if considered for only tones. As such, we consider ramp elements and tones to be equally valuable in the context of statistics of ELF/VLF wave generation.

[20] The right panel of Figure 4 shows the histogram divided up into daytime and nighttime transmissions. The median signal amplitude for nighttime is –13.6 dB-pT and for daytime –11.2 dB-pT. The standard deviation (of the logarithmic value) is 11.4 dB-pT for nighttime and 9.7 dB-pT for daytime. Only a small amount of the variation in signal strength is due to the fact that many frequencies are represented. If only the frequencies between 2000 and 2200 Hz are included, the standard deviation is nearly the same as when all frequencies are included. In general, it appears that daytime signals are stronger on average but that nighttime signals are more variable. We will discuss this more later.

[21] Figure 5 shows the breakdown of ELF/VLF amplitudes as a function of frequency and time of day. The data are binned into 3 h segments and 200 Hz segments. Both tones and ramp elements are included in this analysis, although the ramps somewhat dominate the result since there are about 5 times more ramp elements than tones in the catalog. There are at least 5000 samples in every bin, scattered roughly evenly throughout the 19 months, so there are clearly enough data for these measurements to be fairly reliable.

[22] At the longitude of HAARP, local solar midnight occurs at ∼09:40 UT and local solar noon occurs at ∼21:40 UT. However, the length of the day varies widely between summer and winter at high latitudes. During the summertime, there is a period of several weeks during which the Sun does not set over the lower ionosphere (taken to be 80 km altitude). On the other hand, during the winter, the daytime (even at 80 km altitude) can be only a few hours long. So apart from a few hours surrounding 21:40 UT (which is always daytime), any chosen UT time may correspond to either daytime or nighttime in the lower ionosphere, depending on season. A separate plot was generated in which daytime and nighttime conditions were split apart. The two plots both looked similar to Figure 5.

[23] At all hours of the day, there is a peak in the frequency response corresponding to a cavity resonance. This is the frequency at which the reflection height of the ionosphere (particularly for vertical incidence) is approximately half a free space wavelength. At this frequency, the signal, which is generated in the ionosphere, reflects off the ground

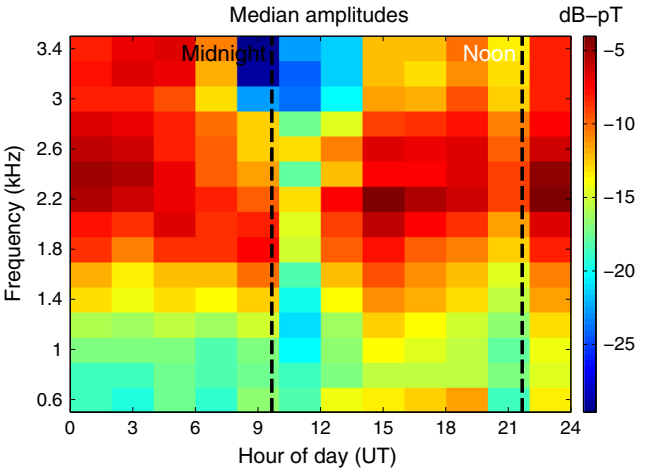

Figure 5. The median amplitude received at Chistochina as a function of time of day and frequency, using both tones and ramp elements. There are at least 5000 points in each bin. Local solar midnight occurs at ∼09:40 UT, and local solar noon occurs at ∼21:40 UT.

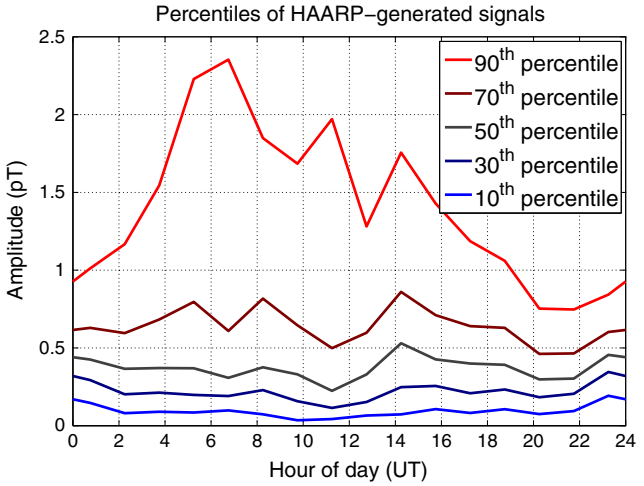

Figure 6. The 90th, 70th, 50th, 30th, and 10th percentile of HAARP-generated amplitudes 1.5–3.5 kHz, as a function of the hour (UT).

and returns to the ionosphere in phase with the generated signal. This reflection height is higher during the nighttime, so the resonance frequency reduces. The peak resonance frequency can be seen to drop toward the middle of the night and then rise again toward the daytime hours.

[24] It has long been the conventional wisdom that nighttime generation is stronger than daytime. This has been in part supported by observations of VLF heating from transmitters and lightning, which can only be made (and only theoretically occur to a noticeable degree) during ionospheric nighttime. In addition, the auroral electrojet strength is typically weaker during daytime. However, the results indicate that higher nighttime generation may not be the case for typical conditions. Past measurements have also reached different conclusions on the question of daytime and nighttime generation. The original [*Getmantsev et al.*, 1974] measurements concluded that generation is stronger during the daytime, but *Tomko* [1981] found that the generation is stronger at night. We have here the first database large enough to clarify definitely.

[25] As seen in Figure 5, there is an apparent valley in the overall frequency response, starting between 06:00 and 09:00 UT and strengthening between 09:00 and 12:00 UT, with the median signal amplitude dropping by ∼10 dB compared to the midday amplitudes. The weakening can be seen prominently not only in the disappearance of the resonance frequency peak but also in the upper frequencies above 3 kHz and lower frequencies 0.8–1.6 kHz. Corresponding closely to midnight, these hours are on average poor for ELF/VLF generation likely due to the Harang discontinuity [*Kamide and Vickrey*, 1983] during which the ionospheric electric field and the ionospheric electrojet currents are known to change direction. It thus appears that in terms of the median generated amplitudes, nighttime may in fact lead to weaker generation in general, at least for HAARPs location and during solar minimum. It can also be observed that generation of the lower frequencies, in particular 500–700 Hz, is noticeably stronger between 12 and 21 UT, corresponding to post midnight and morning hours.

[26] Figure 6 provides a different perspective on the night to day comparison. The median signal amplitude is shown in gray, after combining all the relatively strong frequency bins (1.5–3.5 kHz) from Figure 5 together. Also plotted are the 70th and 90th percentile values (dark red and bright red, respectively), as well as the 30th and 10th percentile values (dark blue and bright blue, respectively). Because the frequency bins are combined, the time bins are 1.5 h long, rather than 3 h, as there are more data in each bin. The dip in the median signal is again apparent between 09:00 and 13:00 UT. But when considering the strongest signal (90th percentile), the best time is actually in the evening, between 04:00 and 10:00 UT, when the 90th percentile values nearly double. So on a select number of days, there is a substantial enhancement in the ELF/VLF generation in the evening. We speculate that this may be the result of sporadic-E layer formation on certain days, which dramatically increases the ionization and HF absorption in the uppermost part of the generation region.

[27] There is a very large disparity in the median signal from one day to the next, as shown by Figure 7, which plots the median amplitudes for each continuous period of HAARP transmission, between 0.5 and 3.5 kHz. The day-to-day variations can easily be 20–30 dB and can change abruptly from 1 day to the next, as demonstrated by Figure 3.

[28] The spread of signals within a single day recording is also wide. Figure 8 shows a summary of how the received amplitude can change as a function of time. We isolated the frequency range 2000–2200 Hz and calculated the amplitude difference between all pairs of transmissions that were separated by less than 5 h. Each column of Figure 8 represents a single probability distribution function for a specific delay time. The time bins are 60 s, and the amplitude difference bins are 0.25 dB. Even with only a 200 Hz band selected, there are enough data so that each time bin has at least 650,000 distinct pairs of transmissions in it.

[29] Figure 8 is closely related to the autocorrelation function of HAARP transmission amplitude as a function of time. If the autocorrelation is high, the signal amplitude

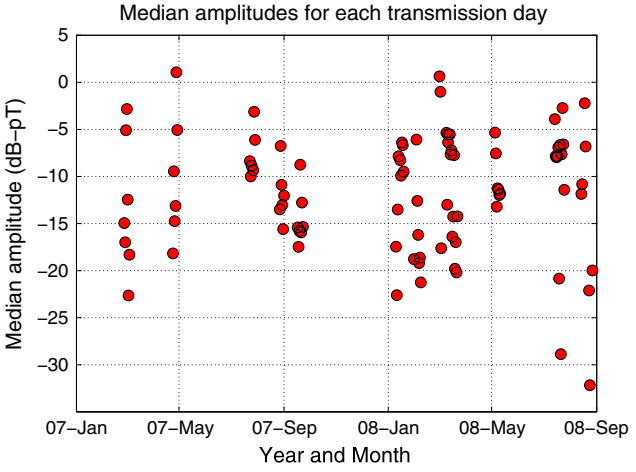

Figure 7. The median amplitudes of each day of HAARP transmission during the 19 month period, for frequencies between 0.5 and 3.5 kHz.

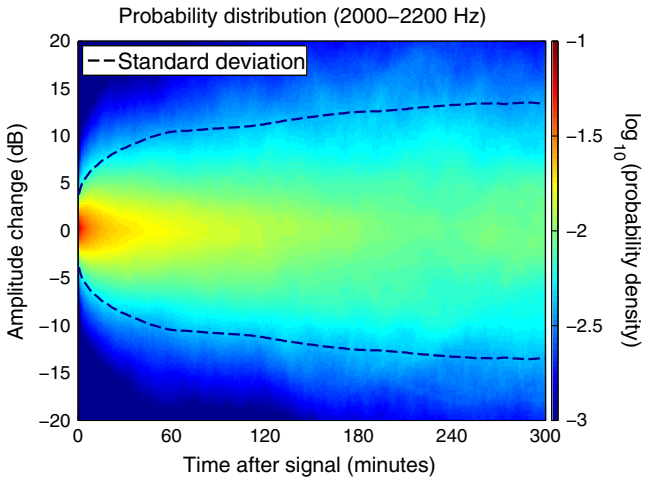

Figure 8. The probability distribution of the signal gain as a function of time. The horizontal axis is delay time between two transmissions, and the vertical axis is the signal change (in dB). Each column represents a single probability distribution function, of transmissions delayed by that amount of time, and at the same frequency (2000–2200 Hz).

will hardly deviate from the original. If the autocorrelation is low, the signal amplitude will be distributed about as broadly as a randomly selected signal amplitude. The black dashed lines show the envelope of 1 standard deviation (of the logarithmic amplitude change), as a function of time. The standard deviation rises quickly over the first 15 min (to 7 dB), then moderately over the next 45 min (reaching ∼11 dB), and then slowly over the next 4 h. These indicate the timescales by which generation conditions can change (finally reaching 13.4 dB). Hence, the 10–11 dB standard deviation observed in Figure 4 is slightly less than the true variability inherent in ELF/VLF generation (13–14 dB), as even long blocks of transmissions (several hours long) contain a lot of self-correlation.

[30] Analyzing the amplitude patterns within a day also allows discussion of slow electron density changes in the lower ionosphere from sustained HF heating, which has been suggested in the past. These changes may result from the increase three-body electron attachment [*Rodriguez and Inan*, 1994], which depletes electrons, and the decreasing electron-ion recombination rate, which can increase electrons [*Rodriguez and Inan*, 1994]. The combined effect sharpens the electron density profile. *Milikh and Papadopoulos* [2007] discuss specifically the impacts from HF heating with HAARP and suggested that electron densities would gradually (over minutes timescale) increase, leading to more efficient generation. *Milikh and Papadopoulos* [2007] propose a preheating technique, where the ionosphere can be first heated continuously, before ELF/VLF generation begins, taking advantage of a more favorable ionosphere. We note that electron density changes from slow chemical affects are distinct from the short-term heating effects that cause the generation, and lead to a patch of the ionosphere acting as a scattering source for VLF radio waves [*Barr et al.*, 1985b].

[31] Prior to the first transmission, the ionosphere is unperturbed and a preheating effect would manifest as a gradual improvement in the signal strength over the first minutes of transmission. However, the natural fluctuations in generation conditions can occur over minutes timescale and may be 10–30 dB, so a single instance of turning on ELF/VLF generation and observing the amplitudes is insufficient to establish whether there is a preheating effect.

[32] However, with the number of days available in this catalog, it is possible to test this statistically. Data from each day are divided into 60 s bins starting from the first recording, covering transmissions between 500 and 3500 Hz. The top panel of Figure 9 shows the median amplitude as a function of time, over the first 3 h of transmission. As shown in the bottom panel, there are enough data for each 60 s bin to have thousands of transmissions, so the results are statistically significant.

[33] Figure 9 shows an increase in the median amplitude at Chistochina by ∼5 dB that occurs gradually over the first ∼30 min of the recording. Figure 9 thus provides some evidence that there may be a preheating effect. We note that we excluded days where there was at least a 10 min stoppage somewhere in the first 3 h (which was about half the days). We also subdivided the 500–3500 Hz band into six 500 Hz sections and found that the warming up of generation conditions was present for all six bins. This excludes the possibility that there may be selection bias from the changing transmission frequency distribution as a function of time. We also investigated whether there is selection bias from the fact that the start times of the many days are not evenly distributed throughout the 24 h, but we did not find any bias. We cannot say at this point if the magnetospherically injected signal is also strengthened by this preheating effect.

[34] This result may constitute the first direct experimental evidence that HF heating (even when modulated) changes the electron density profile in the *D*-region, apparently in a way that improves the generation by ∼5 dB over ∼30 min. The 5 dB intensification is somewhere in between the 7 dB predicted by *Milikh and Papadopoulos* [2007] and the 3 dB changes from simultaneous continuous wave heating discussed by *Moore and Agrawal* [2011]. *Milikh and Papadopoulos* [2007] predicted that the electron

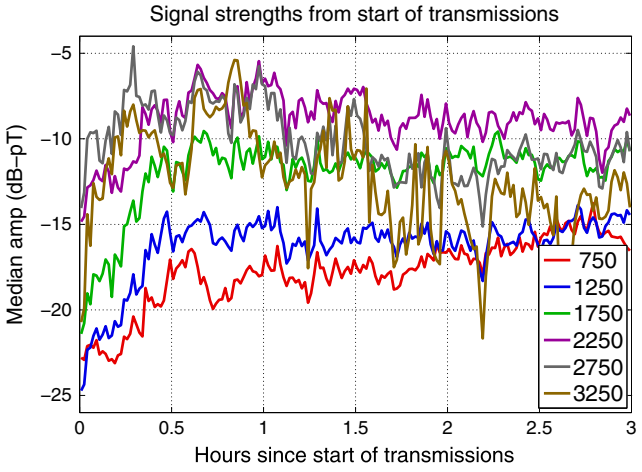

Figure 9. Median amplitudes as a function of the time since transmission began on each day, parametrized by six 500 Hz bins.

density changes would occur over the time span of a few minutes, which is shorter than the 30 min of improving generation conditions observed here. This discrepancy may be explained by the fact that their predictions assume full HAARP power to preheat, whereas modulated HF heating uses only half the HF power. It may also be explained by the uncertain choice of ionosphere parameters in the *Milikh and Papadopoulos* [2007] model.

4. Radiated Power

[35] There have been various estimates of the total power emitted by modulated HF heating. Ground-based estimates usually rely on long-distance detection, where waveguide propagation models are more valid. *Barr et al.* [1985b] estimated 1–2 W of ELF/VLF power on a particularly strong day when the Tromso array radiated 1 MW of HF power, with ELF/VLF powers as small as 100 μW on other days. *Moore et al.* [2007] used distant measurements from the HAARP array operating at a 960 kW level to estimate the ELF source as being between 4 and 32 W, the remaining uncertainty owing to the lack of knowledge of the ionospheric conditions (and resulting attenuation rate). *Platino et al.* [2006] used satellite measurements prior to HAARPs upgrade and estimated a 1–4 W source injected into the magnetosphere. Both long-distance and satellite measurements suffer from the inconsistency of reliable ELF/VLF detection. There have also been theoretical efforts to describe the propagation *Tripathi et al.* [1982].

[36] We use here a three-dimensional theoretical model to try to roughly estimate the radiated power using short-range observations of the magnetic field. We apply a theoretical model of the HF to ELF/VLF conversion process that has been used and validated several times in connection with HAARP-generated ELF/VLF signals [*Cohen et al.*, 2010a, 2011, 2012a, 2012c], so we describe it only briefly here. The model takes as input an ionospheric background condition and a realistic HF radiation pattern from HAARP.

[37] The HF heating is based on earlier work [*Tomko*, 1981; *Rodriguez*, 1994; *Moore*, 2007; *Payne et al.*, 2007], and the HF power flux is injected into the bottom of the ionosphere (at 60 km). The ionosphere is divided into 3-D voxels, 1 km on a side. The HF wave is then propagated upward, including accounting for wave refraction and bending of the wave normal angle [*Moore*, 2007, Ch. 2]. As the wave energy passes through the ionosphere, an energy balance equation is solved that takes into account collisional HF energy absorption and losses by electrons, which are assumed to remain at Maxwellian energy distribution [*Bittencourt*, 2003, p. 165]. The HF absorption comes from the imaginary component of the ionospheric index of refraction, calculated as a function of altitude. Collisional losses by electrons to elastic, rotational, and vibrational states are cataloged by *Rodriguez* [1994, p. 175–178], with the elastic loss rates given by *Banks* [1966], the rotational excitation loss rates given by *Mentzoni and Row* [1963] and *Dalgarno et al.* [1968], and the vibrational excitation loss rates given by *Stubbe and Varnum* [1972]. The remaining HF energy is then propagated upward to the next altitude slab. The HF input is taken in 1 μs time segments so that the nonlinear energy balance equation can be linearized within each time step. The electron temperature at each voxel can be calculated and tracked in time, as a function of the HF energy input (modulated in time and/or space). From the electron temperature, we can calculate the modified electron collision frequency [*Rodriguez*, 1994, p. 176] and therefore the plasma conductivity terms [*Tomko*, 1981, p. 137]. Once the conductivity is tracked as a function of time, the first harmonic (at the fundamental frequency) can be extracted. A background direct current field of 10 mV/m is assumed, yielding a set of current sources embedded in the ionosphere, one in each voxel. Those current sources are placed in a model of ELF/VLF propagation described by *Lehtinen and Inan* [2008, 2009], which provide the fields both in and below the ionosphere.

[38] The ionospheric electron density is taken from the International Reference Ionosphere model, for both summer daytime and winter nighttime conditions. The electron density does not change as a result of HF heating process, since the energy density is too low to ionize, and the electron density changes described by *Milikh and Papadopoulos* [2007] take many minutes to take effect. The geomagnetic field used in the model is taken from the International Geomagnetic Reference Field 2011. The geomagnetic field at HAARP has a declination of ∼22° and a dip angle of ∼16°.

[39] Because ELF/VLF propagation is linear at these strengths (though the HF heating is not), the power is radiated by the source scales with the square of the measured electromagnetic field at some fixed location away from the source. So if generation conditions change and the electrojet magnitude suddenly changes such that quadruple the power at ELF is generated, the magnetic field at a fixed receiver location doubles. So we will utilize the ratio $\frac{B^2_{\text{horiz}}}{P_{\text{ionosphere}}}$ to test the scaling factor between power radiated into the waveguide and the field received at Chistochina. This ratio, however, is a function of frequency, which we must take into account.

[40] Figure 10 shows the results of some calculations using this model. We utilize two different ionospheric profiles (day and night) at frequencies from 1.0 to 3.5 kHz with 250 Hz increments and run the model in each case. We then save the fields everywhere in a 3-D region extending 250 km from HAARP, and from the ground up to 120 km altitude, and calculate the time-harmonic Poynting flux ($\boldsymbol{S} = \boldsymbol{E} \times \boldsymbol{H}^*$) everywhere. Evaluating the Poynting flux also isolates only the radiation term from the ELF/VLF source, rather than the induction terms. To calculate the power into the waveguide, we integrate the Poynting flux in the radial direction (away from HAARP), over the edge of a cylinder at 60 km radius around HAARP, far enough that the HF heating is contained entirely within the cylinder but close enough that waveguide propagation has not dominated the frequency response. The ratio of that power level to the squared horizontal magnetic field at Chistochina is given in the top panel of Figure 10. We also calculate the power flux radiated upward into space by integrating the upward component of the Poynting flux over a disk above the heated region, at 120 km altitude and 250 km radius. This is wide enough to capture most of the upward propagating power [*Cohen et al.*, 2011] and high enough that most of the transionospheric attenuation has already occurred by the time the power reaches 120 km altitude. The ratio of the power to the square horizontal

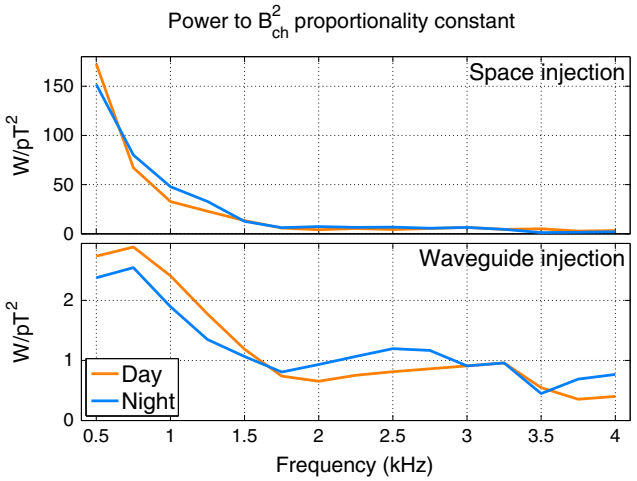

Figure 10. The proportionality constant between the squared horizontal magnetic field at Chistochina and the power (bottom) reaching 60 km distance in the waveguide or (top) reaching 120 km altitude. This is calculated for both daytime (orange) and nighttime (blue) ionospheric conditions and as a function of frequency.

magnetic field at 37 km distance, as a function of frequency, is given in the bottom panel of Figure 10.

[41] At 60 km distance, the effects of the highly variable ionosphere on the propagation below are small, which is why the day and night proportionality constants are fairly similar. At long distances, waveguide propagation efficiency as a function of frequency has an increasingly strong impact on the power and amplitude reaching a certain radius, even if the same magnetic field is measured near to HAARP.

[42] We note that this conversion factor is only valid for this particular configuration of HAARP, using a vertical, narrow beam, at 2.75 or 3.25 MHz, in the range of 1.5–3.0 kHz. Any other distribution of HF power entering the ionosphere changes the distribution of energy between the near field and far field. This includes past measurements of magnetic field made at other HF heating facilities or at HAARP prior to its final upgrade in 2007. For instance, the geometric modulation sweeps, in which the beam is swept in a geometric path with constant power, increase the amplitudes at 700 km distance by 7–11 dB, but at Chistochina, the amplitudes rise only marginally or even decrease [*Cohen et al.*, 2008a]. We also emphasize that in calculating the power that reaches 250 km, we are ignoring any power that is generated but does not reach this distance, as our goal is to estimate only the power that reaches over the horizon and enters the Earth-ionosphere waveguide. So in that sense, it is somewhat different from the power measurements made by earlier workers and yields a smaller power measurement.

[43] We now can convert any given magnetic field measurement at Chistochina to an estimated power level (both in the waveguide and in space) by interpolating as a function of frequency, for either daytime or nighttime.

[44] We can therefore comment on the statistics of power radiated by HAARP and entering the waveguide. Figure 11 shows the cumulative distribution function (CDF) of HAARP-generated ELF/VLF signals for the frequency range 0.5–3.5 kHz, estimated from the measured amplitude values at Chistochina and from the theoretically derived coefficients in Figure 10. The CDF is shown separately for nighttime (blue) and daytime (red) and for waveguide injection (solid lines) and magnetospheric injection (dashed lines).

[45] We first discuss statistics of the waveguide injection signal. The median HAARP-generated power into the waveguide over the 0.5–3.5 kHz frequency band during this 19 month period was 0.056 W for nighttime and 0.09 W for daytime. There is variability in the median as a function of frequency. Table 1 shows the waveguide power at five different percentile values (90%, 70%, 50%, 30%, 10%) and three different frequency ranges (0.5–1.5, 1.5–2.5, and 2.5–3.5 kHz), using the above conversion factor and separately for both daytime and nighttime.

[46] The most powerful daytime transmission in the catalog was transmitted at 2010 Hz on 5 May 2008, at 07:27:07 UT, with an amplitude of just over 20 pT and an estimated waveguide injection power of ∼269 W. The most powerful nighttime transmission was transmitted at 1850 Hz on 12 March 2008, at 07:23 UT, with an amplitude of 17.2 pT and an estimated waveguide injection power of ∼254 Hz.

[47] We note that the ELF/VLF propagation model utilized here is not as well validated for magnetospheric signals, due in large part to a lack of comparative measurements. The model has been validated for steady VLF transmitters close to 20 kHz [*Cohen et al.*, 2012b] but not at the few kHz range. Furthermore, the nonlinear heating generated by the HF heating may impact the propagation of ELF signals through the ionosphere. There are only limited measurements available for HAARP-generated waves injected into the magnetosphere. *Piddyachiy et al.* [2008] and *Cohen et al.* [2011] include a small number of case studies, and a more comprehensive study is presented by *Piddyachiy* [2012], which noted some discrepancies between the model predictions and the observations. *Piddyachiy* [2012] did note that daytime injection into space was more likely than nighttime. In any event, we can not be as certain that the magnetospheric power estimates are correct.

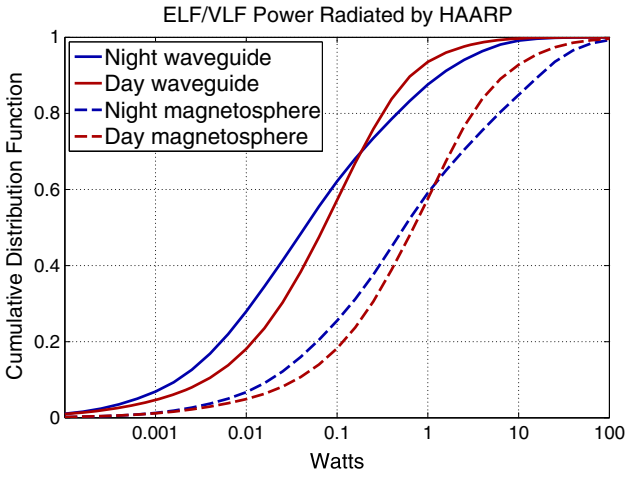

Figure 11. The cumulative distribution function of HAARP-generated signals, both for daytime (red) and nighttime (blue) and for the Earth-ionosphere waveguide (solid) and into the magnetosphere (dashed).

Table 1. Inferred Percentile Power Level for HAARP ELF/VLF Generation Into the Waveguide (60 km Radius) as a Function of Frequency and Time of Day, for 3.25 MHz Vertical AM

	Day 0.5–1.5 kHz	Day 1.5–2.5 kHz	Day 2.5–3.5 kHz	Night 0.5–1.5 kHz	Night 1.5–2.5 kHz	Night 2.5–3.5 kHz
90%	0.60 W	0.97 W	0.96 W	0.78 W	3.26 W	1.92 W
70%	0.17 W	0.27 W	0.28 W	0.15 W	0.41 W	0.21 W
50%	0.071 W	0.10 W	0.10 W	0.039 W	0.086 W	0.048 W
30%	0.026 W	0.036 W	0.034 W	0.012 W	0.021 W	0.011 W
10%	0.0049 W	0.0048 W	0.0037 W	0.0022 W	0.0027 W	0.0015 W

5. Concluding Comments

[48] We note that this entire analysis focuses only on a single configuration of HAARP: narrow vertical beam, amplitude modulation, with 3.25 or 2.75 MHz HF frequency, radiating at full power (close to 3.6 MW). In the introduction, we stated a number of efforts that either have demonstrated or have the potential to eventually demonstrate very significant efficiency improvements in the HF to ELF/VLF conversion process. So the power numbers here do not reflect the limitations of HAARP but rather a baseline for comparison. If generated power is assumed to be boosted by 10 dB, for instance, due to the geometric modulation circle sweep [*Cohen et al.*, 2008a] or more efficient exploitation of the heating and cooling times [*Rietveld et al.*, 1986; *Papadopoulos et al.*, 1990, 2005], then the median power radiated by HAARP to the waveguide, and reaching 250 km, rises to ∼1 W. Future efforts may push this number higher.

[49] It is also worth noting that this 19 month period occurred during an extended solar minimum, so it is very possible that the statistical results presented here would be different and perhaps with stronger generation on average, if taken during an active solar period.

[50] **Acknowledgments.** We thank Mike McCarrick and the HAARP operators for running the HAARP array for these experiments. We thank Ed Kennedy and Paul Kossey for coordinating and arranging the experiments, including the PARS summer schools. We thank Norma and Doyle Traw, of Chistochina Bed and Breakfast, for hosting the ELF/VLF receiver over so many years, and for lots of delicious hot meals after a cold day's work. We thank Jeff Chang for help maintaining the hardware. We thank George Jin, Denys Piddyachiy, for lots of late nights running the real time experiments. We thank Robb Moore for helpful discussions. Finally, we thank Umran Inan for many helpful conversations.

[51] Robert Lysak thanks Robert Moore and an anonymous reviewer for their assistance in evaluating this paper.

References

Agrawal, D., and R. C. Moore (2012), Dual-beam ELF wave generation as a function of power, frequency, modulation waveform, and receiver location, *J. Geophys. Res.*, *117*, A12305, doi:10.1029/2012JA018061.

Banks, P. (1966), Collision frequencies and energy transfer: Electrons, *Planet. Space Sci.*, *14*, 1085–1103.

Barr, R. (1998), The generation of ELF and VLF radio waves in the ionosphere using powerful HF transmitters, *Adv. Space Res.*, *21*(5), 677–687.

Barr, R., and P. Stubbe (1984), ELF and VLF radiation from the "polar electrojet antenna", *Radio Sci.*, *19*(4), 1111–1122.

Barr, R., and P. Stubbe (1991), ELF radiation from the Tromsø "super heater" facility, *Geophys. Res. Lett.*, *18*(6), 1035–1038.

Barr, R., and P. Stubbe (1997), ELF and VLF wave generation by HF heating: A comparison of AM and CW techniques, *J. Atmos. Sol. Terr. Phys.*, *18*(58), 2265–2279.

Barr, R., M. T. Rietveld, H. Kopka, P. Stubbe, and E. Nielsen (1985a), Extra-low-frequency radiation from the polar electrojet antenna, *Nature*, *317*(12), 155–157.

Barr, R., M. T. Rietveld, P. Stubbe, and H. Kopka (1985b), The diffraction of VLF radio waves by a patch of ionosphere illuminated by a powerful HF transmitter, *J. Geophys. Res.*, *90*(A3), 2861–2875.

Barr, R., M. T. Rietveld, P. Stubbe, and H. Kopka (1987), Ionospheric heater beam scanning: A mobile source of ELF/VLF radiation, *Radio Sci.*, *22*(6), 1076–1083.

Barr, R., D. Llanwyn Jones, and C. J. Rodger (2000), ELF and VLF radio waves, *J. Atmos. Sol. Terr. Phys.*, *62*, 1689–1718.

Bittencourt, J. (2003), *Fundamentals of Plasma Physics*, 3rd ed., Springer, New York.

Bortnik, J., U. S. Inan, and T. F. Bell (2006), Temporal signatures of radiation belt electron precipitation induced by lightning-generated MR whistler waves: 1. Methodology, *J. Geophys. Res.*, *111*, A02204, doi:10.1029/2005JA011182.

Cohen, M. B., and U. S. Inan (2012), Terrestrial VLF transmitter injection into the magnetosphere, *J. Geophys. Res.*, *117*, A08310, doi:10.1029/2012JA017992.

Cohen, M. B., M. Gołkowski, and U. S. Inan (2008a), Orientation of the HAARP ELF ionospheric dipole and the auroral electrojet, *Geophys. Res. Lett.*, *35*, L02806, doi:10.1029/2007GL032424.

Cohen, M. B., U. S. Inan, and M. Gołkowski (2008b), Geometric modulation: A more effective method of steerable ELF/VLF wave generation with continuous HF heating of the lower ionosphere, *Geophys. Res. Lett.*, *35*, L12101, doi:10.1029/2008GL034061.

Cohen, M. B., U. S. Inan, M. Gołkowski, and N. G. Lehtinen (2010a), On the generation of ELF/VLF waves for long-distance propagation via steerable HF heating of the lower ionosphere, *J. Geophys. Res.*, *115*, A07322, doi:10.1029/2009JA015170.

Cohen, M. B., U. S. Inan, M. Gołkowski, and M. J. McCarrick (2010b), ELF/VLF wave generation via ionospheric HF heating: Experimental comparison of amplitude modulation, beam painting, and geometric modulation, *J. Geophys. Res.*, *115*, A02302, doi:10.1029/2009JA014410.

Cohen, M. B., U. S. Inan, and E. P. Paschal (2010c), Sensitive broadband ELF/VLF radio reception with the AWESOME instrument, *IEEE Trans. Geosci. Remote Sens.*, *48*(1), 3–17, doi:10.1109/TGRS.2009.2028334.

Cohen, M. B., U. S. Inan, D. Piddyachiy, N. G. Lehtinen, and M. Gołkowski (2011), Magnetospheric injection of ELF/VLF waves with modulated or steered HF heating of the lower ionosphere, *J. Geophys. Res.*, *116*, A06308, doi:10.1029/2010JA016194.

Cohen, M. B., M. Golkowski, N. G. Lehtinen, U. S. Inan, and M. J. McCarrick (2012a), HF beam parameters in ELF/VLF wave generation via modulated heating of the ionosphere, *J. Geophys. Res.*, *17*, A05327, doi:10.1029/2012JA017585.

Cohen, M. B., N. G. Lehtinen, and U. S. Inan (2012b), Models of ionospheric VLF absorption of powerful ground based transmitters, *Geophys. Res. Lett.*, *39*, L24101, doi:10.1029/2012GL054437.

Cohen, M. B., R. C. Moore, M. Golkowski, and N. G. Lehtinen (2012c), ELF/VLF wave generation from the beating of two HF ionospheric heating sources, *J. Geophys. Res.*, *117*, A12310, doi:10.1029/2012JA018140.

Cotts, B. R. T., U. S. Inan, and N. G. Lehtinen (2011), Longitudinal dependence of lightning-induced electron precipitation, *J. Geophys. Res.*, *116*, A10206, doi:10.1029/2011JA016581.

Dalgarno, A., M. B. McElroy, M. H. Rees, and J. C. G. Walker (1968), The effect of oxygen cooling on ionospheric electron temperatures, *Planet. Space Sci.*, *16*, 1371–1380.

Fujimaru, S., and R. C. Moore (2011), Analysis of time-of-arrival observations performed during ELF/VLF wave generation experiments at HAARP, *Radio Sci.*, *46*, RS0M03, doi:10.1029/2011RS004695.

Getmantsev, C. G., N. A. Zuikov, D. S. Kotik, N. A. Mironenko, V. O. Mityakov, Y. A. Rapoport, V. Y. Sazanov, V. Y. Trakhtengerts, and V. Y. Eidman (1974), Combination frequencies in the interaction between high-power short-wave radiation and ionsopheric plasma, *J. Explor. Theor. Phys.*, *20*, 101–102.

Gołkowski, M., U. S. Inan, A. R. Gibby, and M. B. Cohen (2008), Magnetospheric amplification and emission triggering by ELF/VLF waves injected by the 3.6 MW HAARP ionospheric heater, *J. Geophys. Res.*, *113*, A10201, doi:10.1029/2008JA013157.

Gołkowski, M., U. S. Inan, and M. B. Cohen (2009), Cross modulation of whistler mode and HF waves above the HAARP ionospheric heater, *Geophys. Res. Lett.*, *36*, L15103, doi:10.1029/2009GL039669.

Gołkowski, M., U. S. Inan, M. B. Cohen, and A. R. Gibby (2010), Amplitude and phase of nonlinear magnetospheric wave growth excited by the HAARP HF heater, *J. Geophys. Res.*, *115*, A00F04, doi:10.1029/2009JA014610.

Gołkowski, M., M. B. Cohen, D. L. Carpenter, and U. S. Inan (2011), On the occurrence of ground observations of ELF/VLF magnetospheric amplification induced by the HAARP facility, *J. Geophys. Res.*, *116*, A04208, doi:10.1029/2010JA016261.

Gołkowski, M., M. B. Cohen, and R. C. Moore (2013), Modulation of auroral electrojet currents using dual modulated HF beams with ELF phase offset, a potential D-region ionospheric diagnostic, *J. Geophys. Res. Space Physics*, *118*, 2350–2358, doi:10.1002/jgra.50230.

Graf, K. L., U. S. Inan, and M. Spasojevic (2011), Transmitter-induced modulation of subionospheric VLF signals: Ionospheric heating rather than electron precipitation, *J. Geophys. Res.*, *116*, A12313, doi:10.1029/2011JA016996.

Helliwell, R. A., and J. P. Katsufrakis (1974), VLF wave injection into the magnetosphere from Siple Station, Antarctica, *J. Geophys. Res.*, *79*(16), 2511–2518.

Inan, U. S. (1990), VLF heating of the lower ionosphere, *Geophys. Res. Lett.*, *17*(6), 729–732.

Inan, U. S., M. Gołkowski, D. L. Carpenter, N. Reddell, R. C. Moore, T. F. Bell, E. Paschal, P. Kossey, E. Kennedy, and S. Z. Meth (2004), Multi-hop whistler-mode ELF/VLF signals and triggered emissions excited by the HAARP HF heater, *Geophys. Res. Lett.*, *31*, L24805, doi:10.1029/2004GL021647.

Jin, G., M. Spasojevic, M. B. Cohen, U. S. Inan, and N. G. Lehtinen (2011), The relationship between geophysical conditions and ELF amplitude in modulated heating experiments at HAARP: Modeling and experimental results, *J. Geophys. Res.*, *116*, A07310, doi:10.1029/2011JA016664.

Jin, G., M. Spasojevic, M. B. Cohen, and U. S. Inan (2012), Harmonic minimization waveforms for modulated heating experiments at HAARP, *J. Geophys. Res.*, *117*, A11315, doi:10.1029/2012JA018102.

Jin, G., M. Spasojevic, M. B. Cohen, and U. S. Inan (2013), Utilizing nonlinear ELF generation in modulated ionospheric heating experiments for communications applications, *Radio Sci.*, *48*, 61–68, doi:10.1002/rds.20014.

Kamide, Y., and J. F. Vickrey (1983), Relative contribution of ionospheric conductivity and electric field to the auroral electrojets, *J. Geophys. Res.*, *88*(A10), 7989–7996.

Langston, J., and R. C. Moore (2013), High time resolution observations of HF cross-modulation within the *D* region ionosphere, *Geophys. Res. Lett.*, *40*, 1912–1916, doi:10.1002/grl.50391.

Lehtinen, N. G., and U. S. Inan (2008), Radiation of ELF/VLF waves by harmonically varying currents into a stratified ionosphere with application to radiation by a modulated electrojet, *J. Geophys. Res.*, *113*, A06301, doi:10.1029/2007JA012911.

Lehtinen, N. G., and U. S. Inan (2009), Full-wave modeling of transionospheric propagation of VLF waves, *Geophys. Res. Lett.*, *36*, L03104, doi:10.1029/2008GL036535.

McCarrick, M. J., D. D. Sentman, A. Y. Wong, R. F. Wuerker, and B. Chouinard (1990), Excitation of ELF waves in the Schumann resonance range by modulated HF heating of the polar electrojet, *Radio Sci.*, *25*(6), 1291–1298.

Mentzoni, M. H., and R. V. Row (1963), Rotational excitation and electron relaxation in nitrogen, *Phys. Rev.*, *130*, 2312–2316.

Milikh, G. M., and K. Papadopoulos (2007), Enhanced ionospheric ELF/VLF generation efficiency by multiple timescale modulated heating, *Geophys. Res. Lett.*, *34*, L20804, doi:10.1029/2007GL031518.

Moore, R. C. (2007), ELF/VLF wave generation by modulated HF heating of the auroral electrojet, PhD thesis, Stanford University.

Moore, R. C., and D. Agrawal (2011), ELF/VLF wave generation using simultaneous CW and modulated HF heating of the ionosphere, *J. Geophys. Res.*, *116*, A04217, doi:10.1029/2010JA015902.

Moore, R. C., U. S. Inan, T. F. Bell, and E. J. Kennedy (2007), ELF waves generated by modulated HF heating of the auroral electrojet and observed at a ground distance of ∼4400 km, *J. Geophys. Res.*, *112*, A05309, doi:10.1029/2006JA012063.

Moore, R. C., S. Fujimaru, M. Cohen, M. Gołkowski, and M. J. McCarrick (2012), On the altitude of the ELF/VLF source region generated during "beat-wave" HF heating experiments, *Geophys. Res. Lett.*, *39*, L18101, doi:10.1029/2012GL053210.

Papadopoulos, K., C. Chang, P. Vitello, and A. Drobot (1990), On the efficiency of ionospheric ELF generation, *Radio Sci.*, *25*, 1131–1320.

Papadopoulos, K., T. Wallace, G. M. Milikh, W. Peter, and M. McCarrick (2005), The magnetic response of the ionosphere to pulsed HF heating, *Geophys. Res. Lett.*, *32*, L13101, doi:10.1029/2005GL023185.

Payne, J. A., U. S. Inan, F. R. Foust, T. W. Chevalier, and T. F. Bell (2007), HF modulated ionospheric currents, *Geophys. Res. Lett.*, *34*, L23101, doi:10.1029/2007GL031724.

Peter, W. B., and U. S. Inan (2007), A quantitative comparison of lightning-induced electron precipitation and VLF signal perturbations, *J. Geophys. Res.*, *112*, A12212, doi:10.1029/2006JA012165.

Piddyachiy, D. (2012), Propagation of ELF waves generated by an HF ionosperic heater in the Earth's plasma environment, PhD thesis, Stanford University.

Piddyachiy, D., U. S. Inan, T. F. Bell, N. G. Lehtinen, and M. Parrot (2008), DEMETER observations of an intense upgoing column of ELF/VLF radiation excited by the HAARP HF heater, *Geophys. Res. Lett.*, *113*, A10308, doi:10.1029/2008JA013208.

Platino, M., U. S. Inan, T. F. Bell, M. Parrot, and E. J. Kennedy (2006), DEMETER observations of ELF waves injected with the HAARP HF transmitter, *Geophys. Res. Lett.*, *33*, L16101, doi:10.1029/2006GL026462.

Rietveld, M. T., R. Barr, H. Kopka, E. Nielsen, P. Stubbe, and R. L. Dowden (1984), Ionospheric heater beam scanning: A new technique for ELF studies of the auroral ionosphere, *Radio Sci.*, *19*(4), 1069–1077.

Rietveld, M. T., H. Kopka, and P. Stubbe (1986), D-region characteristics deduced from pulsed ionospheric heating under auroral electrojet conditions, *J. Atmos. Terr. Phys.*, *48*(4), 311–326.

Rietveld, M. T., H. P. Mauelshagen, P. Stubbe, H. Kopka, and E. Nielsen (1987), The characteristics of ionospheric heating-produced ELF/VLF waves over 32 hours, *J. Geophys. Res.*, *92*(A8), 8707–8722.

Rodriguez, J. V. (1994), Modification of the Earth's ionosphere by very low frequency transmitters, PhD thesis, Stanford University.

Rodriguez, J. V., and U. S. Inan (1994), Electron density changes in the nighttime *D* region due to heating by very-low-frequency transmitters, *Geophys. Res. Lett.*, *21*(2), 93–96.

Stubbe, P., and W. S. Varnum (1972), Electron energy transfer rates in the ionosphere, *Planet. Space Sci.*, *20*, 1121–1126.

Stubbe, P., H. Kopka, and R. L. Dowden (1981), Generation of ELF and VLF waves by polar electrojet modulation: Experimental results, *J. Geophys. Res.*, *86*(A11), 9073–9078.

Tomko, A. A. (1981), Nonlinear phenomena arising from radio wave heating of the lower ionosphere, PhD thesis, Pennsylvania State Univ., University Park, Penn.

Tripathi, V. K., C. L. Chang, and K. Papadopoulos (1982), Excitation of the Earth-ionosphere waveguide by an ELF source in the ionosphere, *Radio Sci.*, *17*(5), 1321–1326.

Watt, A. D. (1967), *VLF Radio Engineering*, Pergamon Press, New York.